Absolute wavelength measurement of the Lyman-α transitions of hydrogenic Mg^{11+}

G. Hölzer, E. Förster, and D. Klöpfel
X-Ray Optics Group, Institute of Optics and Quantum Electronics, Friedrich-Schiller-University Jena, Max-Wien-Platz 1, D-07743 Jena, Germany

P. Beiersdorfer, G. V. Brown, J. R. Crespo López-Urrutia, and K. Widmann
Department of Physics and Space Technology, Lawrence Livermore National Laboratory, Livermore, California 94550
(Received 23 May 1997)

The wavelengths of the $1s_{1/2}$-$2p_{1/2}$ and $1s_{1/2}$-$2p_{3/2}$ Lyman-α transitions have been measured in hydrogenic Mg^{11+} with an accuracy as high as 24 ppm. The measurement was carried out on an electron-beam ion trap and utilized a quasimonolithic crystal setup absolutely calibrated relative to optical standards. The resulting values for the two transitions were $0.842\,50 \pm 0.000\,04$ and $0.841\,90 \pm 0.000\,02$ nm, respectively. The measurement confirms calculations of the $1s$-$2p$ wavelengths and tests the size of the $1s$ Lamb shift to within 13%. [S1050-2947(98)05502-4]

PACS number(s): 32.30.Rj, 12.20.Fv, 31.30.Jv

I. INTRODUCTION

Hydrogenic ions are the simplest atomic systems and provide the key to understanding and testing fundamental theories. The Dirac equation describes the energy-level separation between the $n=1$ and 2 levels, but small corrections must be added for the nuclear size and the effects of quantum electrodynamics (QED), i.e., for the so-called Lamb shift [1,2]. The corrections are largest for the $1s$ level and affect transitions in the Lyman series the most. Measurements of Lamb shift of the $1s$ level in atomic hydrogen have been made with very high accuracy [3,4], which have provided stringent tests of theory for atomic hydrogen. Small but significant discrepancies with calculations had been noted that persisted until it became possible recently to solve for higher-order, two-loop correction terms [5] in the calculations.

The Lamb shift increases with atomic number as $(\alpha Z)^4$ and it becomes a sizable fraction of the Lyman-α transition energies. In Mg^{11+} the calculated contribution to the $1s$ level is 0.28 eV or 0.02% of the total transition energy [6]. This compares to a mere 0.000 33% in atomic hydrogen [6]. As Z increases, an increasing fraction of the Lamb shift is from the vacuum polarization contribution. Moreover, higher-order terms in αZ become important. As a result, measurements of highly charged hydrogenic ions test different aspects of QED theory and complement the measurements of atomic hydrogen, even though measurements of the $1s$ Lamb shift in highly charged hydrogenic ions have not yet approached the accuracy, either absolute or relative, of the measurements of atomic hydrogen.

Highly charged hydrogenic ions are produced in high-temperature plasma devices and in heavy-ion accelerator facilities, and a number of Lamb shift measurements have been performed using such ion sources. An overview of these measurements involving ions with $Z<30$ is given in Refs. [7–16]. The best accelerator-based measurement was reported with a wavelength accuracy of 5 ppm and used the recoil-ion technique [12]. Because the accuracy of this method was limited by spectator-electron contamination effects, for which it was very difficult to estimate the experimental error, it was subsequently replaced by a method in which bare ions from a heavy-ion accelerator were decelerated and allowed to undergo charge-transfer reactions, resulting in a 41-ppm wavelength measurement of Cl^{16+} [10] and a 13-ppm measurement of Ni^{27+} [16]. The best wavelength measurement from a plasma source, the Alcator tokamak, was reported for Ar^{17+} and achieved an accuracy of 11 ppm [13]. Because the $1s$ Lamb shift in Ni is more than four times larger than the Lamb shift in Cl or Ar, the Ni measurement [16] determines the Lamb shift with the highest relative accuracy (2%) of such measurements in hydrogenic ions to date.

In the following we present a measurement of the transition energy of the Lyman-α transitions in hydrogenic Mg^{11+}, i.e., the $2p_{1/2} \rightarrow 1s_{1/2}$ Lyman-α_1 and the $2p_{3/2} \rightarrow 1s_{1/2}$ Lyman-α_2 transition. The measurement was performed on the Lawrence Livermore National Laboratory electron-beam ion trap (EBIT) facility using an absolutely calibrated quasimonolithic crystal setup for the analysis of the emitted x rays. Absolute calibration of the crystal meant that no reference lines were needed to determine the wavelength of the Lyman-α transitions and that the resulting values were determined in SI units. Moreover, because the EBIT source uses a monoenergetic electron beam to excite the ions and operates in the low-collisional regime with an electron density below 5×10^{12} cm^{-3}, pure Lyman-α transitions are produced unblended with any type of satellite transitions resulting from the presence of spectator electrons in high-n levels. This eliminates the need to account for blending with unknown amounts of satellite transitions, and there is no need for Doppler-shift corrections. In fact, systematic uncertainties in our measurement, which achieved an accuracy as high as 24 ppm, were insignificant. Instead, the limitation of the accuracy of our measurements was dominated by counting statistics.

II. EXPERIMENTAL ARRANGEMENT

The Lawrence Livermore National Laboratory EBIT facility has been described by Levine *et al.* [17]. The facility is

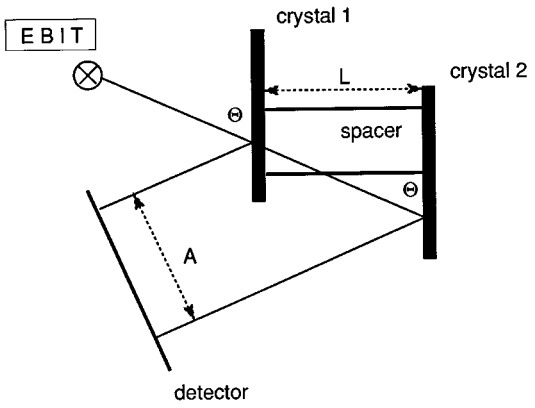

FIG. 1. Schematic of the quasimonolithic setup. The two crystals are separated by a spacer of length L. Bragg reflection of a monochromatic line source results in two images displaced by a distance A on the detector.

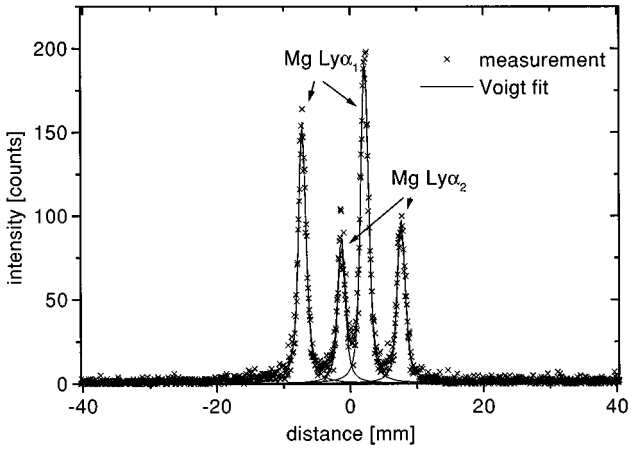

FIG. 2. Spectrum of the $2p_{1/2}\rightarrow 1s_{1/2}$ and $2p_{3/2}\rightarrow 1s_{1/2}$ transition in hydrogenic Mg^{11+}, labeled Mg Lyα_2 and Mg Lyα_1, respectively. Also shown are best fits using Voigt profiles.

well suited for precision spectroscopy because the source is stationary, spatially narrow ($\leqslant 70\ \mu$m), operates in the low-collisional limit ($n_e \leqslant 5\times 10^{12}$ cm^{-3}), and produces highly charged ions with very low ion temperature ($\geqslant 10$ eV) [17–19]. Magnesium is injected into the trap by the metal vapor vacuum arc method [20] and is successively ionized by a 85-mA, 5-keV electron beam. The beam energy is well above the 1762-eV ionization potential of heliumlike Mg^{10+}. Radial ports allow direct line-of-sight access to the trap and observation of the x-ray emission produced by the excitation of the magnesium ions colliding with the electron beam.

The line emission from Mg^{11+} was analyzed using a vacuum crystal spectrometer designed for observing soft-x-ray emission at large Bragg angles and with very high resolution [21]. For the present measurement, the spectrometer employed a quasimonolithic setup with two quartz crystals and a position-sensitive gas proportional counter with a 4-μm thin polypropylene window for recording. The face of the detector was arranged perpendicular to the incoming x rays to avoid line broadening caused by parallax in the 1-cm-deep detector.

A detailed description and characterization of the quasimonolithic crystal setup was given in Ref. [22]. Briefly, it consisted of two $40\times\underline{20}\times 2.5$ mm^3 parallel quartz plates with the orientation (1010) that are mounted onto each side of a quartz glass spacer with length $L=30$ mm and cross section 10×15 mm^2, as illustrated in Fig. 1. The quartz plates are attached to the spacer by optical contact. A vertical displacement of 4 mm allows a simultaneous illumination of both crystal plates.

The quasimonolithic arrangement produces two spectral images on the detector. The separation of the two images depends on the length L of the spacer and the Bragg angle θ of the reflection, i.e., on the wavelength of a spectral line. By measuring the separation A of the two spectral images of a particular x-ray line and knowing L, the angle θ of reflection can be determined, as detailed in Ref. [22]. In fact, the quantities are related by

$$\sin\theta = \sqrt{1-\left(\frac{A}{2L}\right)^2}. \tag{1}$$

From the Bragg law

$$\lambda = 2d\left(\sin\theta - \frac{\delta(\lambda)}{\sin\theta}\right), \tag{2}$$

the wavelength λ of the transition can be determined provided the lattice spacing d of the crystal is known. Here $\delta(\lambda)$ is the wavelength-dependent deviation of the x-ray refraction index in the crystal from unity, typically of order 10^{-4}–10^{-3}. The use of a quasimonolithic setup thus allows a measurement of the wavelength of an x-ray line without the need for x-ray wavelength standards by measuring the displacement of the two spectral images.

The lattice spacing of the crystals had been measured relative to optical standards in a calibration chain that produced a value of $0.425\,495\,6\pm 5\times 10^{-7}$ nm at 293.15 K [22]. Combined with the determination of L to within 1 μm performed in [22], this enables a wavelength determination, in principle, with an accuracy better than 1 ppm. In the present measurement, the measurement accuracy, however, is limited by counting statistics. The uncertainties associated with the value of the lattice spacing or the spacer length are, by comparison, negligibly small.

Because in our method the wavelength of a given line is inferred from the measured displacement of its two images, an accurate calibration of the position-sensitive detector is necessary. We accomplished such a calibration with a collimated, 100-μm-wide ^{55}Fe source mounted on a micrometer drive that was moved in 20 steps, each 1.27 mm apart over the active area of the detector that corresponded to the location of the Mg lines. The dependence of the channel position of the detector versus the source position was fitted with high accuracy by a fourth-order polynomial.

III. SPECTRAL MEASUREMENTS AND ANALYSIS

A spectrum of the $2p_{1/2}\rightarrow 1s_{1/2}$ and $2p_{3/2}\rightarrow 1s_{1/2}$ transitions in Mg^{11+} is shown in Fig. 2. The Bragg angle of the measurement was close to 82°. The two images of the Lyman-α doublet shifted in relation to one another due to the diffraction at the two crystal plates of the quasimonolith are clearly seen in the figure. A total of six spectra were ob-

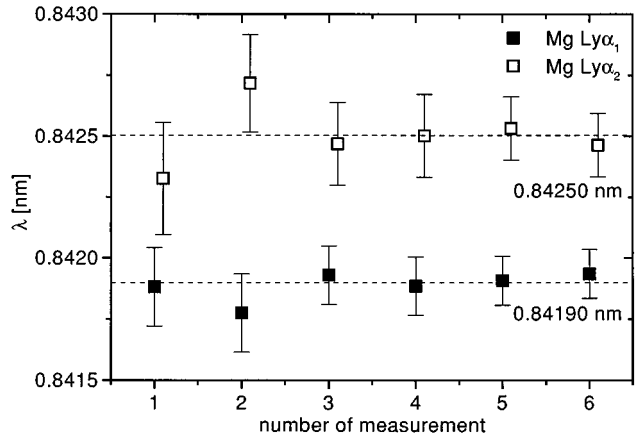

FIG. 3. Results of the analysis of six Mg spectra and weighted average. Error bars represent 1σ confidence limits.

tained, representing a total of about 32 h of actual measurement time.

Each of the four emission lines of the ''double spectrum'' was fitted with a Voigt profile, as illustrated in Fig. 2. The fit procedure used the weighted least-squares method. The fit considerably aided in a precise determination of the peak position. This is especially important because the count rate on an EBIT source is generally small. The error involved with the evaluation of the distances between the peaks thus typically contributes the most to the overall uncertainty. This is demonstrated by the fact that the precision of the peak distance is slightly better for the $2p_{3/2}\rightarrow 1s_{1/2}$ transition than for the $2p_{1/2}\rightarrow 1s_{1/2}$ transition due to the higher number of counts determining the former. A summary of the wavelengths inferred from the measured displacements is given in Fig. 3.

We note that in calculating the wavelengths from the measured displacements we included two important corrections. First, the calculation was done iteratively for an exact correction of the wavelength-dependent refraction. For this, the correction δ was expressed as

$$\delta(\lambda)=\delta_\lambda\lambda+\delta_0. \tag{3}$$

We take $\delta_\lambda=6\times10^{-4}$ nm^{-1} and $\delta_0=-2.61\times10^{-4}$ [23]. This is valid in the wavelength range $0.70\leqslant\lambda\leqslant0.85$ nm, where the linearization error $\Delta\lambda/\lambda\approx2.2\times10^{-7}$ is negligible. Disregarding the refraction correction generally results in systematically too small values for the wavelengths being determined. The differences in this case are about -2×10^{-4} nm.

The other correction we included was that for the thermal expansion of the crystal and thus of its lattice spacing. The temperature of the crystal was monitored with an accuracy of 0.3 K, but differed between measurements by more than 1 K. This temperature influence was corrected by taking into account the temperature expansion coefficient of quartz at 1.37×10^{-5} K^{-1} for any direction perpendicular to the crystallographic c axis [24].

In Table I we summarize the measured wavelengths of the Mg^{11+} Lyman-α lines. The values represent the weighted mean of the six data values shown in Fig. 3. The uncertainty limits mainly represent the statistical uncertainties in the measured peak separations and, to a much lower amount, in the temperature determination. Uncertainties in the crystal parameters are more than one order of magnitude smaller and are insignificant. The uncertainties in our wavelength determination correspond to 1σ confidence limits.

TABLE I. Comparison of measured and calculated wavelengths of the Lyman-α transitions in Mg^{11+}.

Wavelength	Lyman-α_1	Lyman-α_2
measurement	0.841 90 ± 0.000 02	0.842 50 ± 0.000 04
theory[a]	0.841 92	0.842 46

[a]Reference [6].

IV. DISCUSSION

Our measured values are in good agreement with the values calculated by Johnson and Soff [6], as seen in Table I. A better comparison with theory is given if we consider only the Lamb shift contributions. Because the transition energy is the sum of the Dirac energy for a point nucleus and the Lamb shift contribution, the latter can be inferred from our measurement by subtracting the Dirac energy calculated in Ref. [6]. This procedure is possible because the Dirac energy can be calculated for hydrogenic ions with very high accuracy. The results are 0.246 ± 0.044 and 0.351 ± 0.070 eV for the Lamb shift contribution to the Lyman-α_1 and the Lyman-α_2 transition, respectively. Here the uncertainties are the standard 1σ confidence limits. These values need to be com-

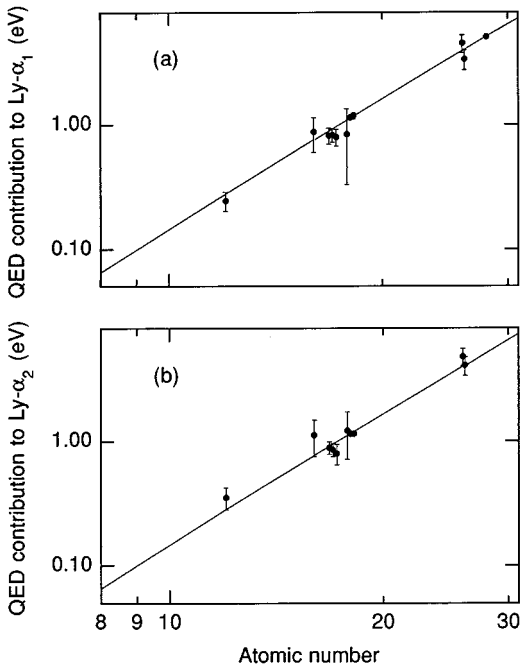

FIG. 4. Comparison of measured and calculated Lamb shift contributions: (a) Lyman-α_1 and (b) Lyman-α_2. Theoretical values (solid lines) are from Ref. [6]. Values for Mg^{11+} are present measurements, for S^{15+} are from Ref. [7], for Cl^{16+} are from Refs. [8–10], for Ar^{17+} are from Refs. [11–13], for Fe^{25+} are from Refs. [14,15], and the measured value for Ni^{27+} is from [16]. Error bars represent 1σ confidence limits for most measurements.

pared to the calculated values 0.281 and 0.283 eV [6], respectively. The weighted average of our measurements is 0.276 ± 0.037 eV. This tests the calculated average of 0.282 eV to within 13%.

A comparison of the inferred Lamb shift contributions to the Lyman-α_1 and the Lyman-α_2 transitions with theory is given in Fig. 4. This comparison includes all known measurements in the range $8 \leqslant Z \leqslant 30$. The comparison verifies theory within the experimental uncertainties. It also shows that our Mg measurement represents the only measurement of Lamb shift contributions in the range $\approx 0.08-0.80$ eV.

The present measurement made use of an absolutely calibrated quasimonolithic crystal setup for absolute wavelength measurements. Past wavelength measurements on the EBIT have been made relative to reference lines from other highly charged ions generated *in situ*. Typically, hydrogenic reference lines were used for this purpose. This procedure evidently precludes measuring the wavelengths of hydrogenic lines. The present technique thus opens the possibility to perform absolute measurements of any x-ray transition provided the appropriate crystals are available. This is important because Lamb shift measurements have not been performed for most elements. The EBIT technique allows such measurements virtually without the systematic uncertainties, such as Doppler shifts or satellite contamination, that have limited the accuracy of many such measurements from other sources. Unlike tokamak or accelerator-based measurements, which typically have very high count rates, the accuracy of our present measurement was limited mainly by the counting statistics. The accuracy can be improved in the future to values below 10 ppm, as the technique is further developed to include higher count rate efficiencies of the spectrometer and higher x-ray from the EBIT, resulting in 4–5 times longer effective exposure times.

ACKNOWLEDGMENTS

This work was performed in part by Lawrence Livermore National Laboratory under the auspices of the U.S. Department of Energy under Contract No. W-7405-ENG-48.

[1] W. E. Lamb and R. C. Retherford, Phys. Rev. **72**, 241 (1947).
[2] H. A. Bethe, Phys. Rev. **72**, 339 (1947).
[3] M. Weitz, A. Huber, F. Schmidt-Kaler, D. Leibfried, and T. W. Hänsch, Phys. Rev. Lett. **72**, 328 (1994).
[4] S. Bourzeix, B. de Beauvoir, F. Nez, M. D. Plimmer, F. de Tomasi, L. Julien, F. Biraben, and D. N. Stacey, Phys. Rev. Lett. **76**, 384 (1996).
[5] K. Pachuki, Phys. Rev. Lett. **72**, 3154 (1994).
[6] W. R. Johnson and G. Soff, At. Data Nucl. Data Tables **33**, 405 (1985).
[7] L. Schleinkofer, F. Bell, H.-D. Betz, G. Trollmann, and J. Rothermel, Phys. Scr. **25**, 917 (1982).
[8] P. Richard, M. Stockli, R. D. Deslattes, P. Cowan, R. E. La Villa, B. Johnson, K. Jones, M. Meron, R. Mann, and K. Schartner, Phys. Rev. A **29**, 2939 (1984).
[9] E. Källne, J. Källne, P. Richard, and M. Stöckli, J. Phys. B **17**, L115 (1984).
[10] R. D. Deslattes, R. Schuch, and E. Justiniano, Phys. Rev. A **32**, 1911 (1985).
[11] J. P. Briand, J. P. Mossé, P. Indelicato, P. Chevallier, D. Girard-Vernhet, and A. Chetioui, Phys. Rev. A **28**, 1413 (1983).
[12] H. F. Beyer, R. D. Deslattes, F. Folkmann, and R. E. Villa, J. Phys. B **18**, 207 (1985).
[13] E. S. Marmar, J. E. Rice, E. Källne, J. Källne, and R. E. La Villa, Phys. Rev. A **33**, 774 (1986).
[14] J. P. Briand, M. Tavernier, P. Indelicato, R. Marrus, and H. Gould, Phys. Rev. Lett. **50**, 832 (1983).
[15] J. D. Silver, A. F. McClelland, J. M. Laming, S. D. Rosen, G. C. Chandler, D. D. Dietrich, and P. O. Egan, Phys. Rev. A **36**, 1515 (1987).
[16] H. F. Beyer, P. Indelicato, K. D. Finlayson, D. Liesen, and R. D. Deslattes, Phys. Rev. A **43**, 223 (1991).
[17] M. A. Levine, R. E. Marrs, J. N. Bardsley, P. Beiersdorfer, C. L. Bennett, M. H. Chen, T. Cowan, D. Dietrich, J. R. Henderson, D. A. Knapp, A. Osterheld, B. M. Penetrante, M. B. Schneider, and J. H. Scofield, Nucl. Instrum. Methods Phys. Res. B **43**, 431 (1989).
[18] P. Beiersdorfer, V. Decaux, S. Elliott, K. Widmann, and K. Wong, Rev. Sci. Instrum. **66**, 303 (1995).
[19] P. Beiersdorfer, J. R. Crespo López-Urrutia, E. Förster, J. Mahiri, and K. Widmann, Rev. Sci. Instrum. **68**, 1077 (1997).
[20] I. G. Brown, J. E. Galvin, R. A. MacGill, and R. T. Wright, Appl. Phys. Lett. **49**, 1019 (1986).
[21] P. Beiersdorfer, J. R. Crespo López-Urrutia, E. Förster, J. Mahiri, and K. Widman, Rev. Sci. Instrum. **68**, 1077 (1997).
[22] D. Klöpfel, G. Hölzer, E. Förster, and P. Beiersdörfer Rev. Sci. Instrum. **68**, 3669 (1997).
[23] δ_λ and δ_0 are calculated with the computer code DIXI developed by G. H. using the wavelength-dependent corrections for the atomic scattering factors from B. L. Henke, E. M. Gullikson, and J. C. Davies, At. Data Nucl. Data Tables **54**, 181 (1993).
[24] J. C. Brice, Rev. Mod. Phys. **57**, 105 (1985).